Influence of adhesive layer properties on laser-generated ultrasonic waves in thin bonded plates*

Sun Hong-Xiang(孙宏祥)[a)b)†], Xu Bai-Qiang(许伯强)[a)], Zhang Hua(张 华)[a)], Gao Qian(高 倩)[a)], and Zhang Shu-Yi(张淑仪)[b)]

[a)] *Faculty of Science, Jiangsu University, Zhenjiang* 212013, *China*
[b)] *Laboratory of Modern Acoustics, Ministry of Education, and Institute of Acoustics, Nanjing University, Nanjing* 210093, *China*

(Received 12 January 2010; revised manuscript received 9 June 2010)

This paper studies quantitatively the generation of Lamb waves in thin bonded plates subjected to laser illumination, after considering the viscoelasticity of the adhesive layer. The displacements of such plates have been calculated in the frequency domain by using the finite element method, and the time domain response has been reconstructed by applying an inverse fast Fourier transform. Numerical results are presented showing the normal surface displacement for several configurations: a single aluminum plate, a three-layer bonded plate, and a two-layer plate. The characteristics of the laser-generated Lamb waves for each particular case have been investigated. In addition, the sensitivity of the transient responses to variations of material properties (elastic modulus, viscoelastic modulus, and thickness) of the adhesive layer has been studied in detail.

Keywords: laser applications, surface acoustic waves, adhesive bonds, finite element method
PACS: 43.35.+d, 42.62.–b, 83.60.Bc, 02.70.Dh **DOI:** 10.1088/1674-1056/20/1/014302

1. Introduction

Due to its noncontact feature and the ability of broadband signal generation, the technique of laser-generated Lamb waves has demonstrated its great potential for nondestructive evaluation and characterisation of the sheet materials in industry. For that reason, many previous works can be found on the study of laser-generated Lamb waves in various media such as plates or pipes made of either single or stratified, isotropic or anisotropic, elastic or viscoelastic materials.[1−7] These works help to understand the behaviour of Lamb waves, thus making it possible to optimise the method of particular modes for detecting specific defects in tested plates. However, among all the media of investigation, adhesive bonded plates, made of two sheet metals plus a viscoelastic adhesive layer in between, have rarely been considered. These types of structures are increasingly used in the modern aerospace and automobile industries for their high mechanical performances and low weights. Aging, plus thermal and mechanical loadings are only a few of the mechanisms that could lead to failure or damage of these adhesive bonds. As a result, maintenance and reliability are crucial subjects. Usually the adhesive bond layer itself is not accessible or visible. The choice of Lamb waves for testing such structures has been motivated due to their great potentiality for quickly testing quite a long range of the specimen. Nevertheless, before an non destructive testing process gets set up, a signal generated by a laser source in such a system with a viscoelastic adhesive layer must be well understood.

In adhesive bonded plates, the features of laser-generated Lamb waves depend not only on the properties of the adhesive layer, but also on those of the top and bottom layers, so that Lamb waves become increasingly more difficult to interpret as the structural system becomes more complex. Rokhlin and Wang[8] have investigated the equivalent boundary conditions for a thin epoxy resin layer between solids, and they presented that the bonding layer can be approximated well by spring model for a very thin lower density layer. Heller *et al.*[9] have combined laser ultrasound techniques with two-dimensional Fourier transformation to characterise the stiffness of adhesive bonds,

*Project supported by the National Natural Science Foundation of China (Grant No. 11074125), the Major Project of the Natural Science Foundation of the Jiangsu Higher Education Institutions of China (Grant No. 10KJA140006), the Natural Science Foundation of the Jiangsu Higher Education Institutions of China (Grant No. 08KJB140003), and the Student Research Foundation of the Jiangsu University, China (Grant Nos. 2010074 and 09A101).
†Corresponding author. E-mail: jsdxshx@ujs.edu.cn
© 2011 Chinese Physical Society and IOP Publishing Ltd

and they experimentally measured transient Lamb waves in layered plates to study the effect of the adhesive bond on the dispersion curves of these systems. Cheng *et al.*[10] have simulated the laser-generated ultrasonic waves in an elastic isotropic bonded plate in the Hankel and Laplace transform domain by using the Thompson transfer matrix approach, and then they obtained the signal in the time domain through a numerical inverse transform where the laser irradiation was dealt with a surface force. Liu *et al.*[11] have utilised a laser induced grating technique to generate narrow band surface waves in an epoxy-bonded copper-aluminum layered structure, and then they introduced an inverse algorithm based on the simplex method to determine the bonding thickness as well as the elastic properties of the bonding layer. All these works show that the laser ultrasonic wave testing technique is a powerful tool in the characterisation of the bonding layer quality in bonded plates. However, the bonding layers are considered as purely elastic materials in the above publications, and little work has been published so far on the investigation for laser-generated Lamb waves in such plates, taking account of the material viscoelasticity. Constitutive relations developed in the Fourier domain and using complex moduli which represent that the viscoelastic material properties allow the dynamic behaviour of these media to be properly described,[12−14] and several cases of the propagation of ultrasonic waves in layered plates made of viscoelastic materials have been modeled successfully[15,16] Nevertheless, these works were restricted to generating and receiving ultrasonic waves with air-coupled transducers, which can not obtain ultrasound signals with high frequency and good spatial resolution.

Due to the complexity of the generation and propagation of Lamb waves in bonded plates with viscoelastic bonding layers, numerical methods will be much more suitable in dealing with the complicated processes, especially in processes involving various parameters. The finite element (FE) method, solving the problems in the frequency domain,[17] has many advantages. First of all, it is versatile due to its flexibility in modeling complicated geometries and the feasibility of obtaining full field numerical solutions.[18,19] In addition, compared with classical FE method[20−23] which uses numerical routines to produce time marching solutions, thus requiring hundreds or thousands of iterative calculations, the FE method proposed here needs much less time and memory consuming since it consists in solving the dynamic equations of equilibrium for a limited number of frequencies which constitute the frequency spectrum of a temporal excitation. Furthermore, complex moduli representing the viscoelastic property introduced in this method can effectively solve the problem of laser-generated Lamb wave propagation in a viscoelastic bonding layer In this article, the FE method is adopted to establish the model of laser-generated Lamb waves in a thin bonded plate with a viscoelastic adhesive layer in the frequency domain, and the time domain responses are then reconstructed by applying an inverse fast Fourier transform (FFT). The sensitivity of the transient responses to variations of material properties of the viscoelastic adhesive layer is studied quantitatively.

2. Basic theory and numerical method

2.1. Plane strain theory

We consider an infinite three-layer bonded plate that consists of homogeneous, isotropic, and linearly either elastic or viscoelastic layers, each with a thickness of h_k ($k = 1, 2, 3$). The coordinates x, y, and z of the model are chosen to be parallel to the principal axis of the bonded plate, with y being the optical axis of laser pulse irradiation, as shown in Fig. 1. The motion is assumed to take place in three dimensions (x, y, z), and the displacements in the x, y, and z directions are u_k, v_k, and w_k, respectively. The pulsed laser line source is assumed to focus along the line of z-axis on the top surface of the bonded plate, and produces non-null displacements in both directions x and y only, see Fig. 2. With the plane strain conditions ($\varepsilon_{xz,k} = \varepsilon_{yz,k} = \varepsilon_{zz,k} = 0$), the displacement w_k and all derivatives with respect to z vanish, and the two-dimensional governing equation in the frequency domain is written as follows:

$$\begin{cases} C^*_{11,k}\dfrac{\partial^2 \tilde{u}_k}{\partial x^2} + C^*_{66,k}\dfrac{\partial^2 \tilde{u}_k}{\partial y^2} + (C^*_{12,k} + C^*_{66,k})\dfrac{\partial^2 \tilde{v}_k}{\partial x \partial y} + \rho_k \omega^2 \tilde{u}_k = 0, \\ C^*_{22,k}\dfrac{\partial^2 \tilde{v}_k}{\partial y^2} + C^*_{66,k}\dfrac{\partial^2 \tilde{v}_k}{\partial x^2} + (C^*_{12,k} + C^*_{66,k})\dfrac{\partial^2 \tilde{u}_k}{\partial x \partial y} + \rho_k \omega^2 \tilde{v}_k = 0, \end{cases} \tag{1}$$

where $(\tilde{u}_k, \tilde{v}_k)$ is the Fourier transform of the displacement vector, ρ_k is the density, the subscript $k = 1, 2, 3$ represents the kth layer, and ω is the angular frequency. The moduli $C^*_{ij,k}$ in Eq. (1) can be defined to be complex quantities if the material is viscoelastic: $C^*_{ij,k} = C'_{ij,k} + \mathrm{i}\, C''_{ij,k}$, the real part represents the elastic moduli and the imaginary part its viscoelastic moduli.

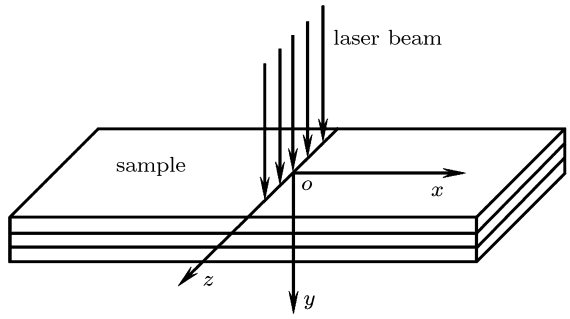


Fig. 1. Schematic diagram for laser irradiating the sample.

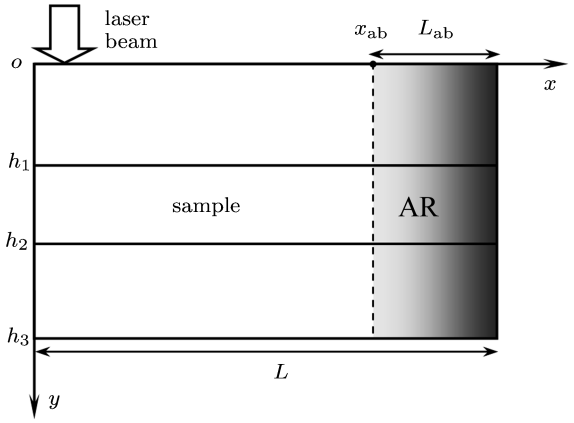


Fig. 2. Cross section of the sample.

2.2. Numerical method

For wave propagation calculated in the frequency domain, the above partial differential equation, Eq. (1), must be written in the following FE-code form:[24]

$$\nabla \cdot (\boldsymbol{c}\nabla \tilde{\boldsymbol{U}}_{\boldsymbol{k}}) - \boldsymbol{a}\tilde{\boldsymbol{U}}_{\boldsymbol{k}} = 0, \tag{2}$$

where the symbol ∇ is the vector differential operator defined as $\nabla = (\partial/\partial x, \partial/\partial y)$, and the variable $\tilde{\boldsymbol{U}}_{\boldsymbol{k}}$ to be determined corresponds to the vector $(\tilde{u}_k,\ \tilde{v}_k)$. Then, the coefficient $\boldsymbol{c}$ is a 2×2 matrix composed of four sub-matrices, that is

$$\boldsymbol{c}_{11} = \begin{pmatrix} C^*_{11,k} & 0 \\ 0 & C^*_{66,k} \end{pmatrix}, \quad \boldsymbol{c}_{12} = \begin{pmatrix} 0 & C^*_{12,k} \\ C^*_{66,k} & 0 \end{pmatrix},$$

$$\boldsymbol{c}_{21} = \begin{pmatrix} 0 & C^*_{66,k} \\ C^*_{12,k} & 0 \end{pmatrix}, \quad \boldsymbol{c}_{22} = \begin{pmatrix} C^*_{66,k} & 0 \\ 0 & C^*_{22,k} \end{pmatrix},$$

and the coefficient $\boldsymbol{a}$ is a 2×2 matrix given by

$$\boldsymbol{a} = \begin{pmatrix} -\rho_k\omega^2 & 0 \\ 0 & -\rho_k\omega^2 \end{pmatrix}.$$

The boundary conditions are expressed as the Neumann type, which corresponds to an excitation source on the laser illuminative region and to a stress-free boundary on the top and bottom surface of the bonded plate. The boundary conditions are expressed as

$$\boldsymbol{n} \cdot (\boldsymbol{c}\nabla \tilde{\boldsymbol{U}}_{\boldsymbol{k}}) = \boldsymbol{g}, \tag{3}$$

where $\boldsymbol{n}$ is the unit vector normal to the surface, and the term $\boldsymbol{g}$ represents the excitation source on the boundary. In the case of a stress-free boundary $\boldsymbol{g} = 0$. In addition, the stress tensors and displacements are considered to be continuous at the interfaces of the adjacent layers, and the initial displacement and velocity are null.

2.3. Absorbing region

When simulating the propagation in the frequency domain, it is mandatory to eliminate the reflections at the edges. A viscoelastic absorbing region (AR) is simulated with a fictitious material for which the viscoelastic moduli $C''^{\mathrm{AR}}_{ij,k}$ are increased progressively to absorb any waves entering this region. In a layered plate, the imaginary part of the complex moduli is regularly increased at the right-hand-side of each layer of the plate (Fig. 2). The following function is used to define the imaginary part of the complex moduli involved in the AR:[16]

$$\begin{aligned} &C''^{\mathrm{AR}}_{ij,k} = C''_{ij,k} + A\left(\frac{|x_{\mathrm{ab}} - x|}{L_{\mathrm{ab}}}\right)^3 C'_{ij,k}, \\ &L - L_{\mathrm{ab}} < x \le L, \\ &(C''_{ij,k} = 0 \quad \text{if material is elastic}), \end{aligned} \tag{4}$$

where $C'_{ij,k}$ and $C''_{ij,k}$ represent the material properties in the domain of propagation (DP), i.e. the domain of interest for the generation and propagation, $C''^{\mathrm{AR}}_{ij,k}$ are the material properties in the AR, x_{ab} is the position of the interface separating the DP and the AR, and A is a coefficient that may be adjusted to minimise the acoustic impedance mismatch between the DP and the AR. To present the effect of the AR on the propagation, we investigate a case of a 0.1 mm, 30 mm

long, aluminum plate, with symmetric mode (S_0) and asymmetric mode (A_0) coexisting at a frequency equal to 0.5 MHz by using the AR. The predicted amplitude of the normal surface displacement along the propagation direction is shown in Fig. 3.

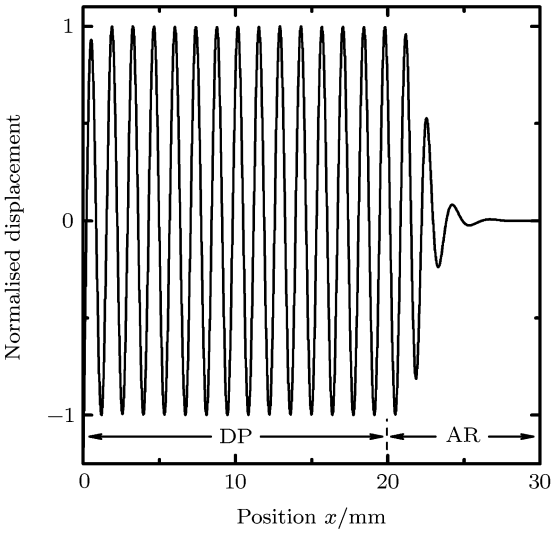


Fig. 3. Surface normalised normal displacement of an aluminum plate at 0.5 MHz along the x direction.

As expected, in the AR, i.e., from $x = 20$ to 30 mm, the amplitude drastically diminishes and tends towards zero, this indicates that no wave propagates backwards along the DP to influence the incident wave.

3. Numerical results and discussions

3.1. Materials and laser parameters

Based on the theories described above, the laser-generated Lamb waves are calculated in a three-layer bonded plate of two aluminum plates joined together with an adhesive bonding layer (the middle layer), and the thicknesses of the two aluminum plates are the same. The pulsed laser source is located at the position $x = 0$ mm on the top (aluminum) layer, just as it would in a real application. Typical properties of these materials used in the calculation are listed in Table 1.[25]

Table 1. Mechanical properties of materials used in models.

	$\rho/(\mathrm{g{\cdot}cm^{-3}})$	C_{11}^*/GPa	C_{22}^*/GPa	C_{12}^*/GPa	C_{66}^*/GPa
aluminum	2.78	112	112	58	27
adhesive	1.1	7+ i0.21	7+ i0.21	4.8+ i0.144	1.1+ i0.033

Harmonic waves can be generated by using pulsed laser techniques.[26,27] In this work, the laser source is replaced by an equivalent stress and is given by[28]

$$f(t) = \frac{2}{\alpha\sqrt{2\pi}} \exp\left[-\frac{(t-t_0)^2}{2\alpha^2}\omega_{\mathrm{c}}^2\right] \sin(\omega_{\mathrm{c}} t), \quad 0 \le t \le t_{\mathrm{d}}, \tag{5}$$

where α is a parameter controlling the pulse width, t_0 determines the pulse delay time, and $\omega_{\mathrm{c}} = 2\pi f_{\mathrm{c}}$ is the centre angular frequency of the pulse. Here, we choose $\alpha = 1.2$, $t_0 = 5$ μs, and $f_{\mathrm{c}} = 0.5$ MHz. Figures 4(a) and 4(b) show the time history of the chosen excitation source and its frequency spectrum, $f(t)$ and $F(f)$, respectively.

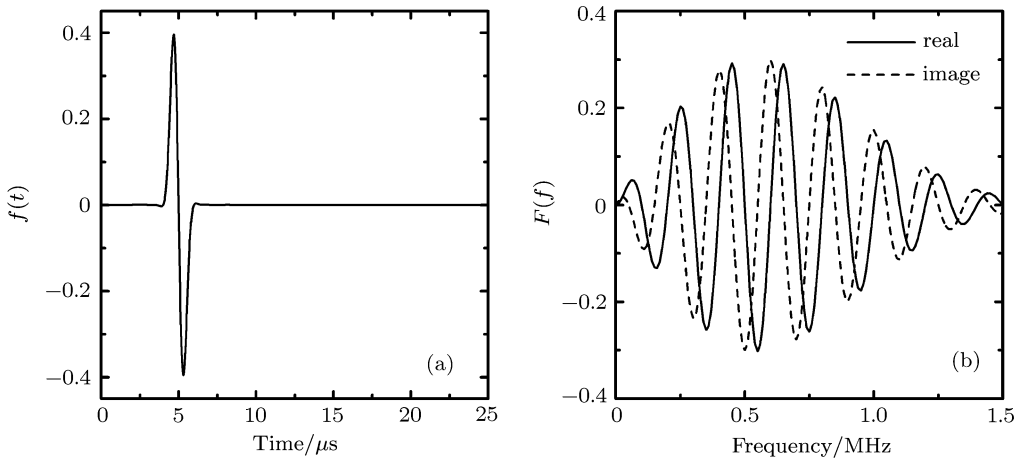


Fig. 4. (a) Time history of the excitation source and (b) its frequency spectrum.

3.2. Model of simulation

Spatial resolution of the FE model is critical for the convergence of the numerical results. Choosing an adequate element size is very important for the stability and accuracy of the solution. In the calculation, triangular element with quadratic behaviour is used to mesh the plate where propagation is produced, and the element size L_e is 50 μm, which satisfies the criterion suggested by Ref. [29].

$$L_e \leq \frac{1}{10}\frac{C}{f_{max}}, \tag{6}$$

where C represents the surface acoustic wave speed of the aluminum plate, and f_{max} is the highest frequency in the ultrasonic fields.

The frequency spectrum $F(f)$ is used as the excitation source of the FE model in the frequency domain. As seen in Fig. 4(b), the frequency content of the pulse is confined to $0 \leq f \leq 1.5$ MHz, and 150 frequency components are enough to represent this frequency spectrum. In the calculation, a number of 150 stationary analysis runs for the corresponding force amplitudes are performed, with the method of using a single parametric solution in the frequency domain. Complex displacements are predicted in both directions x and y for the whole set of nodes. Temporal responses are then reconstructed for several node positions by applying an inverse FFT for the set of complex displacements predicted for the 150 frequency components of the input.

3.3. Numerical results and discussion

The influences of the adhesive layer are shown in Figs. 5(a) and 5(b) which compare the three-layer bonded system with a single aluminum plate of the same total thickness (100 μm). In this case, the three-layer bonded system under consideration is a 30 mm long three-layer plate, where the top and bottom layers are 40 μm thick aluminum plates and the middle layer is a 20 μm thick adhesive. The time domain traces at a source-to-receiver distance of 10 mm are shown in Fig. 5(a). Good agreement can be found in terms of the characteristics of the modes S_0 and A_0 propagating through comparing the features of the waveforms in the single aluminum plate calculated by the FE model in the frequency domain with those of the numerical results in Ref. [30]. It presents that the lower frequency components of the modes S_0 and A_0 are dominant in such a thin plate. The initial arrival shows the S_0 mode, followed later by the dispersive A_0 mode with larger displacement amplitude which means that the energy of Lamb waves is mainly in the A_0 mode. The presence of the adhesive layer causes a clear decrease in the velocity and an increase in the amplitude of both the S_0 and A_0 modes. This is particularly true for the A_0 mode, which is more sensitive than the S_0 mode. In addition, it shows clearly that the adhesive layer causes a decrease in the dispersion of the A_0 mode. The effects of the adhesive layer are also shown in the dispersion curve in Fig. 5(b). It can be found that the adhesive layer causes a marked decrease in the velocity of both modes and in the dispersion of the A_0 mode.

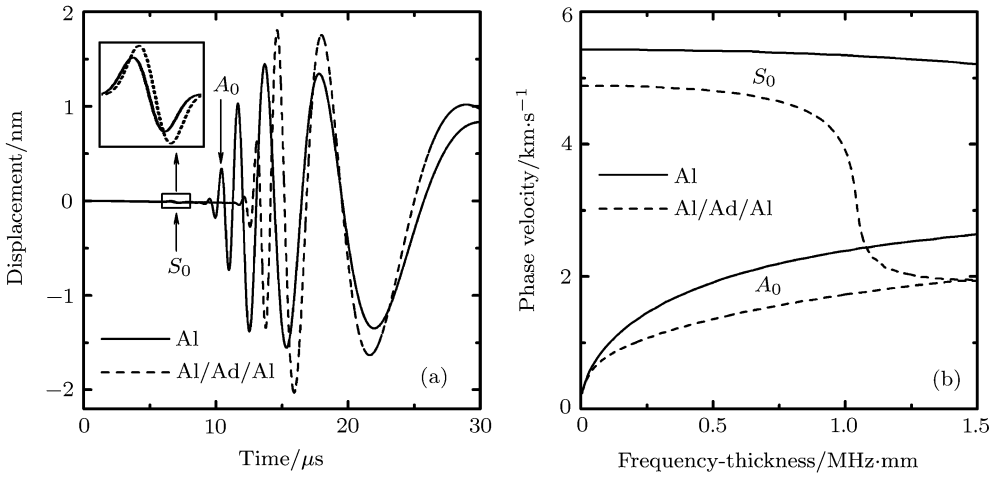


Fig. 5. (a) Surface normal displacement and (b) dispersion curve of the three-layer (Al/Ad/Al) plate are compared to the signal aluminum plate of the same total thickness.

To evaluate unknown material properties of a layer structure from measured data by using an inverse technique requires a sensitivity analysis of the signals to variations of the material parameters. It can then be determined whether the unknown parameters can be extracted. As a first example, to study the effects of the viscoelasticity of the adhesive layer on the transient responses, the viscoelastic rate m of the adhesive layer is gradually increased by varying the imaginary parts of the complex moduli $C^*_{ij} = C'_{ij} + m(\mathrm{i}\, C''_{ij})$, from 0 to 2 of the nominal values given in Table 1. The transient responses at the top surfaces with a source-to-receiver distance of 15 mm are presented in Figs. 6(a) and 6(b). Comparison of the waveforms in the purely elastic adhesive layer (dashed lines) with those in the viscoelastic adhesive layer (solid lines) shows that the amplitudes of both modes decrease gradually with increasing values of m, this indicates that the attenuation of Lamb waves is related to the viscoelasticity of the adhesive layer. Moreover, it is shown that the sensitivity of all the modes in the laser-generated Lamb waves is different from each other. As shown in Fig. 6, the amplitude of the A_0 mode is much more sensitive than that of the S_0 mode. In addition, comparison of the various frequency signals (t = 17.18, 19.44, 22.24, 27.72 μs) of the A_0 mode shows the amplitude of the higher frequency signals varies much more than that of the lower frequency ones with increasing values of m. This phenomenon is clearly presented in Fig. 7. This suggests that even for the A_0 mode itself the sensitivity is different with respect to the frequency, where the higher frequency signals vary much more than the lower frequency ones. It is because the attention in higher modes is in general higher than that in the lower modes.

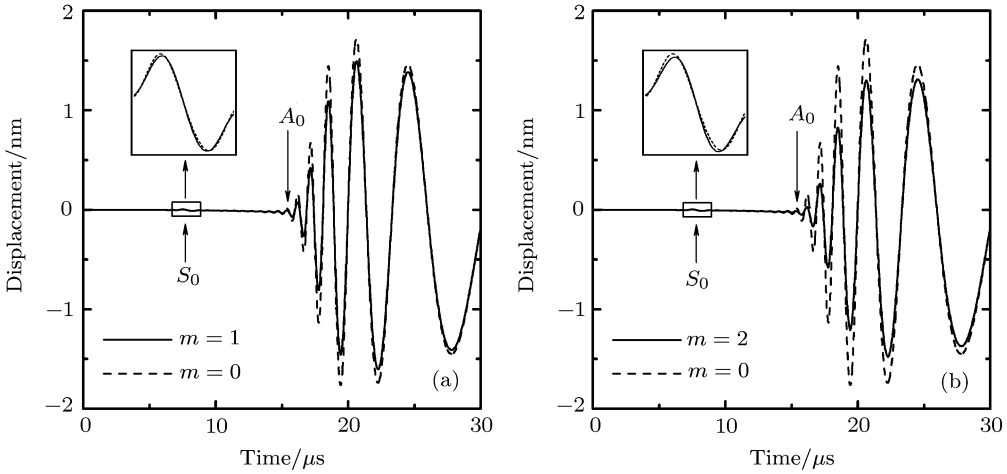


Fig. 6. Sensitivity of the signal to the variation of the viscoelastic rate m of the adhesive layer in a three-layer plate with Al/Ad/Al configuration.

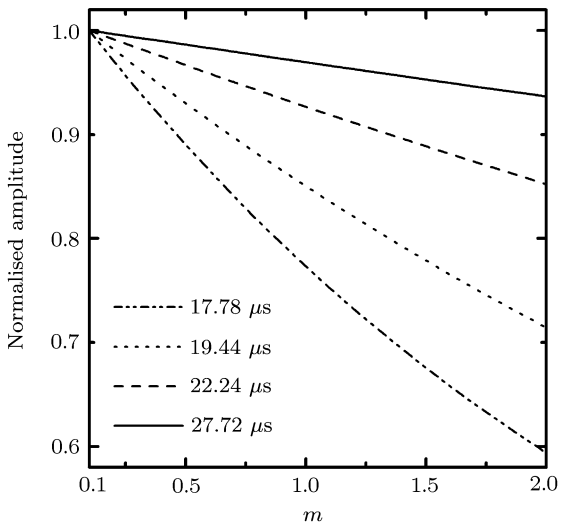


Fig. 7. Normalised amplitudes of various frequency signals versus the material viscoelastic rate m.

We also calculated the normal surface displacements with variations in the elastic moduli of the adhesive layer. In this case, the complex moduli of the adhesive layer are set to be $C^*_{ij} = nC'_{ij} + \mathrm{i}\, C''_{ij}$, and the elastic rate n is varied from 0.8 to 1.2. The responses with a source-to-receiver distance of 15 mm are shown in Figs. 8(a) and 8(b), where the solid lines represent the variations (n = 0.8, 1.2) and the dashed lines represent the original values (n = 1). It clearly shows that the velocities of both modes increase gradually with the increase of the elastic rate n. Such a phenomenon results from the fact that the velocity of Lamb waves is related to the elastic modulus of the adhesive layer. The greater the elastic modulus is, the faster the wave velocity is. It can also

be observed from Fig. 8 that the velocity of the A_0 mode is much more sensitive than the S_0 mode. In addition, comparison of the same frequency signals of the A_0 mode in Fig. 8 clearly presents that the velocity of the higher frequency components increases more quickly than that of the lower frequency ones with increasing values of n, which is also shown in Fig. 9.

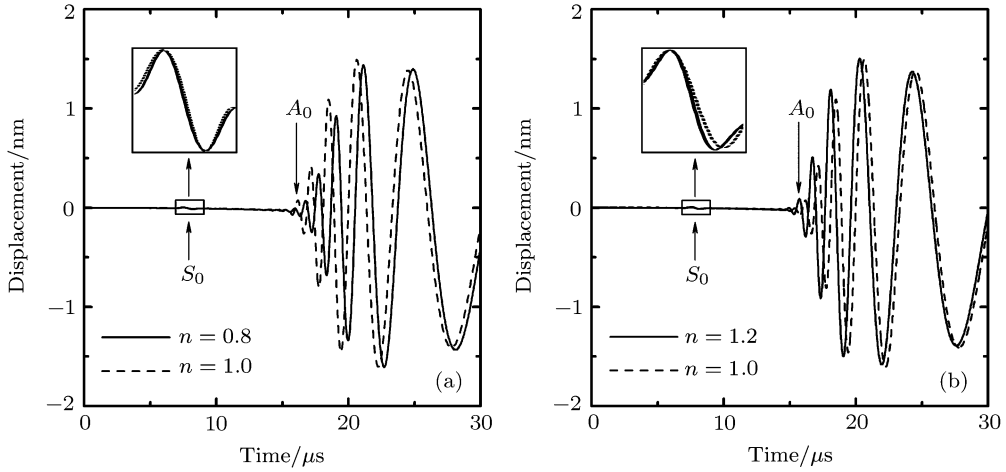


Fig. 8. Sensitivity of the signal to the variation of the elastic rate n of the adhesive layer in a three-layer plate with Al/Ad/Al configuration.

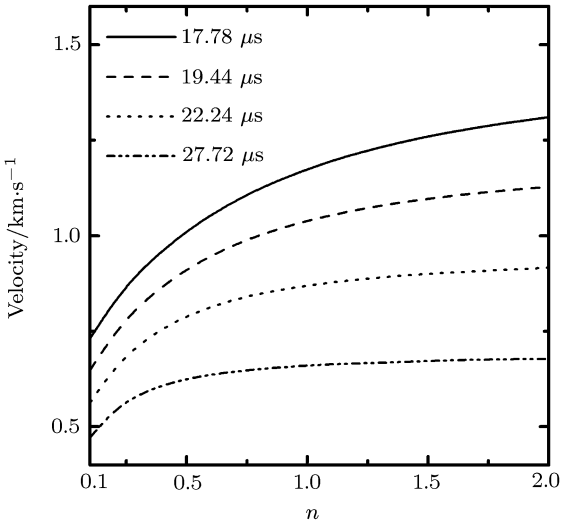


Fig. 9. Velocities of various frequency signals versus the material elastic rate n.

To investigate the influences of the adhesive layer thickness on the laser-generated Lamb waves, the normal surface displacements are calculated in the three-layer plates with an adhesive layer thickness h of 10, 20, and 30 μm, respectively, where the thickness of the top and bottom aluminum plates corresponds to 45, 40, and 35 μm, for ensuring that the total thicknesses of the layered plates are the same. The transient responses with a source-to-receiver distance of 10 mm are shown in Figs. 10(a) and 10(b). It can be seen that the velocities of the S_0 and A_0 modes decrease gradually with the increase of the adhesive layer thickness h. This is because the velocity of Lamb waves is getting close to that in a signal adhesive plate with increasing values of h. We can also see the phenomenon that the velocities of the higher frequency signals of the A_0 mode vary much more sensitively than the lower frequency signals of the A_0 model and the S_0 mode. In addition, comparison of the various frequency signals (t = 12.57, 13.76, 15.92, 21.63 μs) of the A_0 mode (h = 20 μm) and the S_0 mode in Fig. 10 clearly shows that the amplitudes of the higher frequency components decrease with the increase of h, while the amplitudes of the lower frequency ones and the S_0 mode increase gradually. It indicates that the energy of the higher frequency signals is converted to the lower frequency ones and the S_0 mode gradually decreases with the increase of h. Moreover, it clearly presents that the amplitude of the higher frequency signals (t = 12.57, 15.92 μs) varies much more than that of the lower frequency ones (t = 13.76, 21.63 μs). This phenomenon is also shown in Fig. 11. So, the higher frequency signals of the A_0 mode can be used to extract the thickness of the adhesive layer in an effective way.

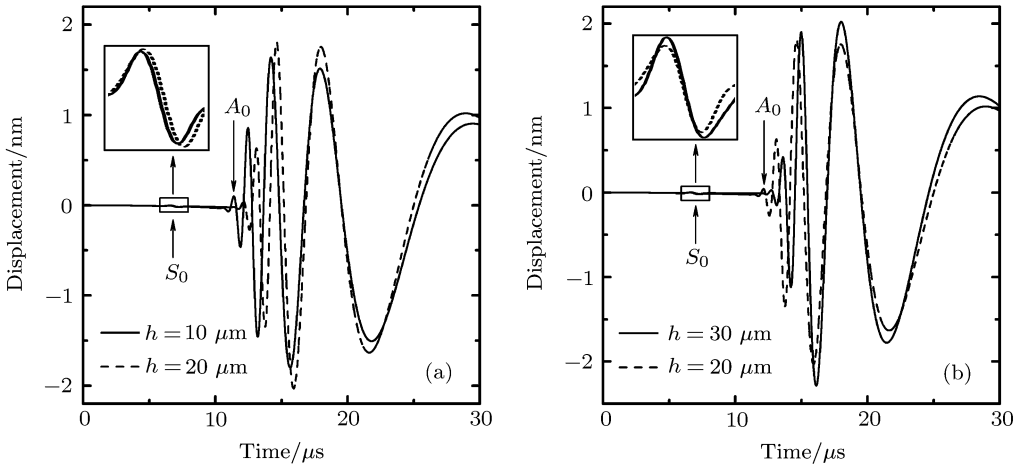


Fig. 10. Sensitivity of the signal to the variation of the thickness h of the adhesive layer in a three-layer plate with Al/Ad/Al configuration.

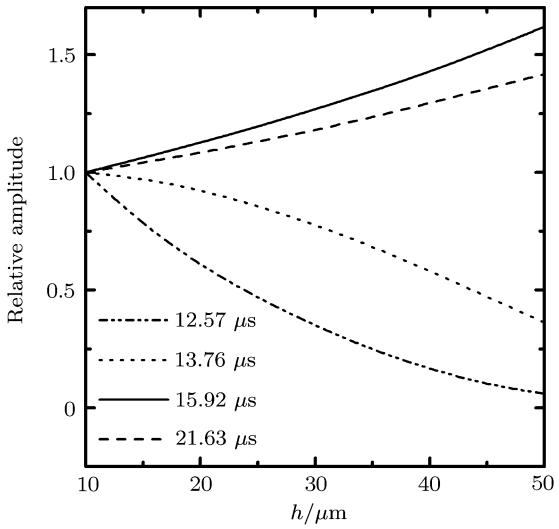


Fig. 11. Relative amplitudes of various frequency signals versus the adhesive layer thickness h.

Next, the normal surface displacements for the case of a two-layer plate with a source-to-receiver distance of 10 mm are also calculated. For a two-layer plate, calculations have been made for the following configuration: adhesive/aluminum. Again the thickness of the surface adhesive layer h is set to be 10, 20, and 30 μm, respectively, while the aluminum plate 90, 80, and 70 μm correspondingly for obtaining the same total thicknesses of the systems as those in Fig. 10. The time domain traces are presented in Fig. 12. Numerical results clearly show that the characteristics of the lower frequency signals of the A_0 mode vary much more sensitively than those in the three-layer bonded systems (Fig. 10) with the increase of h, which leads support to the conclusion that the lower frequency modes are primarily sensitive to the properties of the top layer.

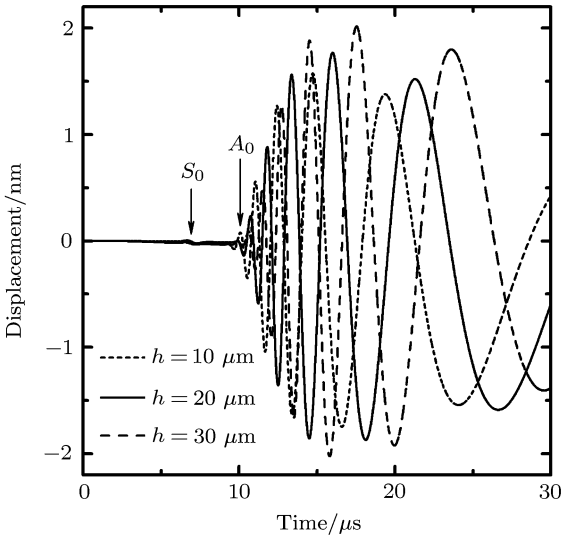


Fig. 12. Sensitivity of the signal to the variation of the thickness h of the adhesive layer in a two-layer plate with adhesive/aluminum configuration.

4. Conclusions

The generation of ultrasound in a thin bonded plate subjected to laser illumination has been studied quantitatively, taking account of the material viscoelasticity. The normal surface displacements of the bonded plate have been calculated in the frequency domain by using the FE method, and the time domain response has been reconstructed by applying an inverse FFT. Several numerical results are calculated giving normal displacement in the following configurations: a single aluminum plate, a three-layer bonded plate and a two-layer plate. The characteristics of

the laser-generated transient responses for these cases have been studied. In addition, the sensitivity of the transient responses to variations of material properties (C''_{ij}, C'_{ij}, and h) of the adhesive layer has been investigated in detail. The numerical analyses indicate that the FE model can decide the modes, which are generated by a laser source in a layered system with a viscoelastic bonding layer, and it can also be used to determine the sensitivity that the generated modes cause changes in elastic modulus, viscoelastic modulus and thickness of the bonding layer. The further investigation to determine the properties of the bonding layers by using an inverse method is in progress.

References

[1] Viktorov I A 1967 *Rayleigh and Lamb Waves: Physical Theory and Applications* (New York: Plenum)
[2] Spicer J B, McKie A D W and Wagner J W 1990 *Appl. Phys. Lett.* **57** 1882
[3] Wu T T and Liu Y H 1999 *Ultrasonics* **37** 405
[4] Cheng J C and Zhang S Y 1999 *Appl. Phys. Lett.* **74** 2087
[5] Cheng J C, Wang T H and Zhang S Y 2000 *Appl. Phys.* B: *Lasers Opt.* **70** 57
[6] Al-Qahtani H and Datta S K 2004 *J. Appl. Phys.* **96** 3645
[7] Prada C, Balogun O and Murray T W 2005 *Appl. Phys. Lett.* **87** 194109
[8] Rokhlin S I and Wang Y J 1991 *J. Acoust. Soc. Am.* **89** 503
[9] Heller K, Jacobs L J and Qu J 2000 *NDT & E Int.* **33** 555
[10] Cheng A, Murry T W and Achenbach J D 2001 *J. Acoust. Soc. Am.* **110** 848
[11] Liu Y H, Wu T T and Lee C K 2002 *J. Acoust. Soc. Am.* **111** 2638
[12] Christensen R M 1971 *Theory of Viscoelasticity: An Introduction* (New York: Academic)
[13] Fluge W 1975 *Viscoelasticity* (Berlin: Springer-Verlag)
[14] Ferry J D 1980 *Viscoelastic Properties of Polymers* (New York: Wiley)
[15] Castaings M and Hosten B 2003 *J. Acoust. Soc. Am.* **113** 2622
[16] Hosten B and Castaings M 2005 *J. Acoust. Soc. Am.* **117** 1108
[17] Sun H X, Xu B Q, Wang J J, Xu G D, Xu C G and Wang F 2009 *Acta Phys. Sin.* **58** 6344 (in Chinese)
[18] Cheng Y, Huang Q J and Liu X J 2008 *Chin. Phys.* B **17** 4273
[19] Huang B, Zhang Y L, Zhang D and Gong X F 2010 *Chin. Phys.* B **19** 054302
[20] Xu B Q, Shen Z H, Ni X W and Lu J 2004 *J. Appl. Phys.* **95** 2116
[21] Shen Z H, Xu B Q, Ni X W and Lu J 2004 *J. Phys.* D: *Appl. Phys.* **37** 2364
[22] Zhao Y, Shen Z H, Lu J and Ni X W 2007 *Acta Phys. Sin.* **56** 321 (in Chinese)
[23] Yuan L, Shen Z H, Ni X W and Lu J 2007 *Acta Phys. Sin.* **56** 7058 (in Chinese)
[24] COMSOL *Multiphysics User's Guide* Version 3.5 - http://www.comsol.com/
[25] Castaings M and Lowe M 2008 *J. Acoust. Soc. Am.* **123** 696
[26] Matsuda Y, Richardson C J K and Spicer J B 2001 *Appl. Phys. Lett.* **79** 2288
[27] Hernandez C M, Murray T W and Krishnaswany S 2002 *Appl. Phys. Lett.* **80** 691
[28] Mukdadi O M and Datta S K 2004 *Rev. Prog. Quant. Nondestr. Eval.* **23** 238
[29] Schubert F, Koehler B and Peiffer A 2001 *J. Comput. Acoust.* **9** 1127
[30] Xu B Q, Shen Z H, Ni X W and Lu J 2004 *J. Appl. Phys.* **95** 2109